

Electronic Supplementary Information

Post-Functionalization Modification as a Modular Strategy for Size-Selective Fluorescence Response of Single-Walled Carbon Nanotubes to Polycyclic Aromatic Hydrocarbons

Srestha Basu,^{a,b,c} Dominik Just,^d Adi Hendler-Neumark,^a Dawid Janas,^d and Gili Bisker^{*a,e,f,g,h}

^a School of Biomedical Engineering, Faculty of Engineering, Tel Aviv University, Tel Aviv 6997801, Israel

^b Biophysical Sciences Group, Saha Institute of Nuclear Physics, 1/AF Bidhannagar, Kolkata 700064, India

^c Chemical Sciences Division, Homi Bhabha National Institute, Mumbai 400094, India

^d Department of Chemistry, Silesian University of Technology, B. Krzywoustego 4, 44-100 Gliwice, Poland

^e Center for Physics and Chemistry of Living Systems, Tel Aviv University, Tel Aviv 6997801, Israel

^f Center for Nanoscience and Nanotechnology, Tel Aviv University, Tel Aviv 6997801, Israel

^g Center for Light-Matter Interaction, Tel Aviv University, Tel Aviv 6997801, Israel

^h Sagol School of Neuroscience, Tel Aviv University, Tel Aviv 6997801, Israel

Email: bisker@tauex.tau.ac.il

Table of Contents

1. Synthesis of PFO-BPy6,6' and PFO-FH for purification of SWCNTs and characterization thereof	2
2. Quantum yield calculations	3
3. Supporting data	4
4. References	19

1. Synthesis of PFO-BPy6,6' and PFO-FH for purification of SWCNTs and characterization thereof

The synthesis of conjugated polymers was conducted according to a Suzuki coupling procedure reported by us earlier.¹ In brief, organoboron derivative (9,9-di-*n*-alkylfluorene-2,7-diboronic acid bis(pinacol)ester, 0.763 mmol, 1.00 mol. eq.) and dibromo derivative (9,9-dihexyl-2,7-dibromofluorene or 6,6'-dibromo-2,2'-dipyridyl, 0.763 mmol, 1.00 mol. eq.) were added to the high-pressure glass reaction vessel. The reactor was then filled with a mixture of 1M Na₂CO₃ solution (12 mL) and toluene (12 mL). Three drops of Aliquat 336, serving the role of the phase transfer catalyst, were added. To remove oxygen, the mixture was purged with argon for 30 min, and subsequently, Pd(PPh₃)₄ (0.019 mmol, 0.025 eq.) was added to catalyze the coupling procedure. The reaction mixture was stirred at 80°C for 3 days. Afterward, it was cooled down, diluted with 250 mL of chloroform, and washed 4× with 150 mL of water. The organic phase was collected and dried with anhydrous MgSO₄, which was then removed by filtration. The collected material was evaporated and dissolved in chloroform to dissolve all solid particles. The final product was precipitated with methanol. The resulting polymers were collected by filtration, washed 2× with 50 mL of freezing methanol, and, finally, 2× with 50 mL of ice-cold acetone. The macromolecular parameters of the obtained polymers were confirmed using size exclusion chromatography (SEC), and their structures were determined with ¹H NMR spectroscopy (Figure S1).

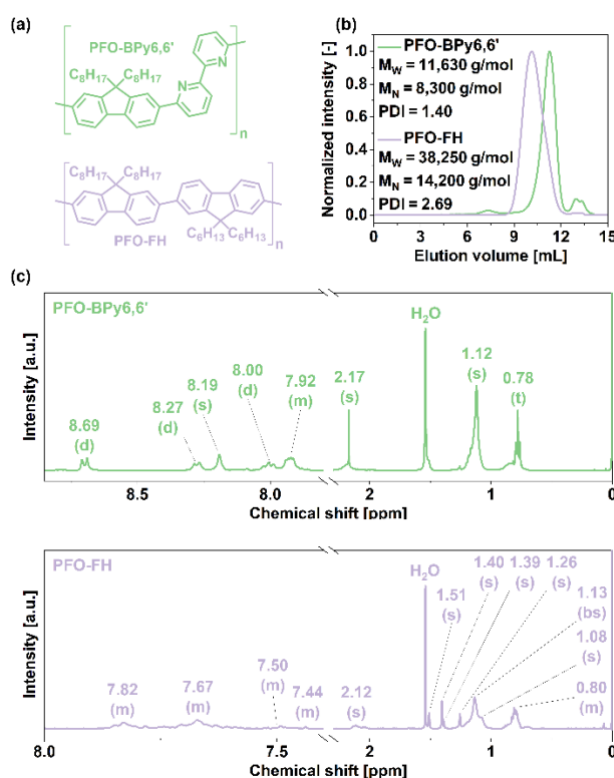


Figure S1: (a) Chemical structures of PFO-BPy6,6' and PFO-FH. (b) SEC chromatograms and macromolecular parameters of the synthesized polymers (M_w – weight average molecular weight, M_n – number average molecular weight, PDI – polydispersity index). (c) ¹H NMR spectra of the indicated polymers.

The molecular characteristics of PFO-BPy6,6' and PFO-FH were measured using Size Exclusion Chromatography (SEC, Agilent 1260 Infinity, Agilent Technologies). The setup was equipped with an isocratic pump, autosampler, degasser, a thermostatic box for columns, and a differential refractometer MDS RI Detector. Linear polystyrene standards were used for the calibration, enabling the determination of the SEC-calculated molecular weight. A pre-column guard (5 μ m, 50 \times 7.5 mm) and two columns (PLGel 5 μ m MIXED-C 300 \times 7.5 mm and PLAGel 5 μ m MIXED-D 300 \times 7.5 mm) were used for separation of the analytes. The measurements were conducted using CHCl₃ (HPLC grade) as the solvent (flow rate of the solvent: 0.8 mL/min, room temperature: 30°C). ¹H NMR spectra of the synthesized polymers (Figure S1c) were registered in CDCl₃ using a Varian Unity Inova spectrometer operating at 400 MHz. ¹H-chemical shifts were measured in δ (ppm), using the CDCl₃ residual peak positioned at δ 7.26.²

2. Quantum yield calculations

The relative quantum yield (QY) of PFM-(6,5) SWCNTs before and after PAH addition was determined using Rhodamine B as a reference standard, which has a known QY of 65% in toluene. Similarly, the QY of PFM-(7,5) SWCNTs was calculated using Cy5 as the standard, with a reported QY of 20% in water. The following equation was used for the quantum yield calculations:

$$QY_s = QY_r \times (I_s/I_r) \times (A_r/A_s) \times (\eta_s^2/\eta_r^2)$$

where QY_s and QY_r are the QY of the sample and the reference, respectively, I_s and I_r are the areas under the emission curves of the sample and the reference, respectively, A_s and A_r are the absorption of the sample and the reference at their respective excitation wavelengths, and η_s and η_r are the refractive indexes of the solvents containing the sample and the reference, respectively. Note that, per standard procedure,³ while refractive index corrections were accounted for, other solvent-related factors may influence the QY and were not explicitly considered. Therefore, the QY calculation for the PFM-(7,5) SWCNTs in toluene serves as an estimate, as the reported QY of the Cy5 standard is based on measurements in water, and contributions beyond refractive index differences were not taken into account.

3. Supporting data

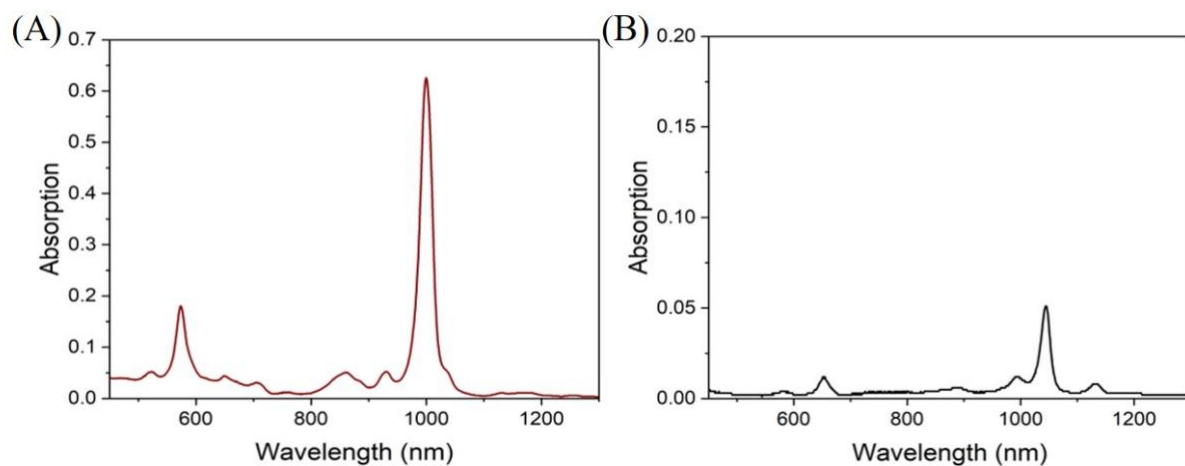


Figure S2: UV-vis-NIR absorption spectra of (A) PFO-BPy6,6' (6,5) SWCNTs and (B) PFO-FH (7,5) SWCNTs.

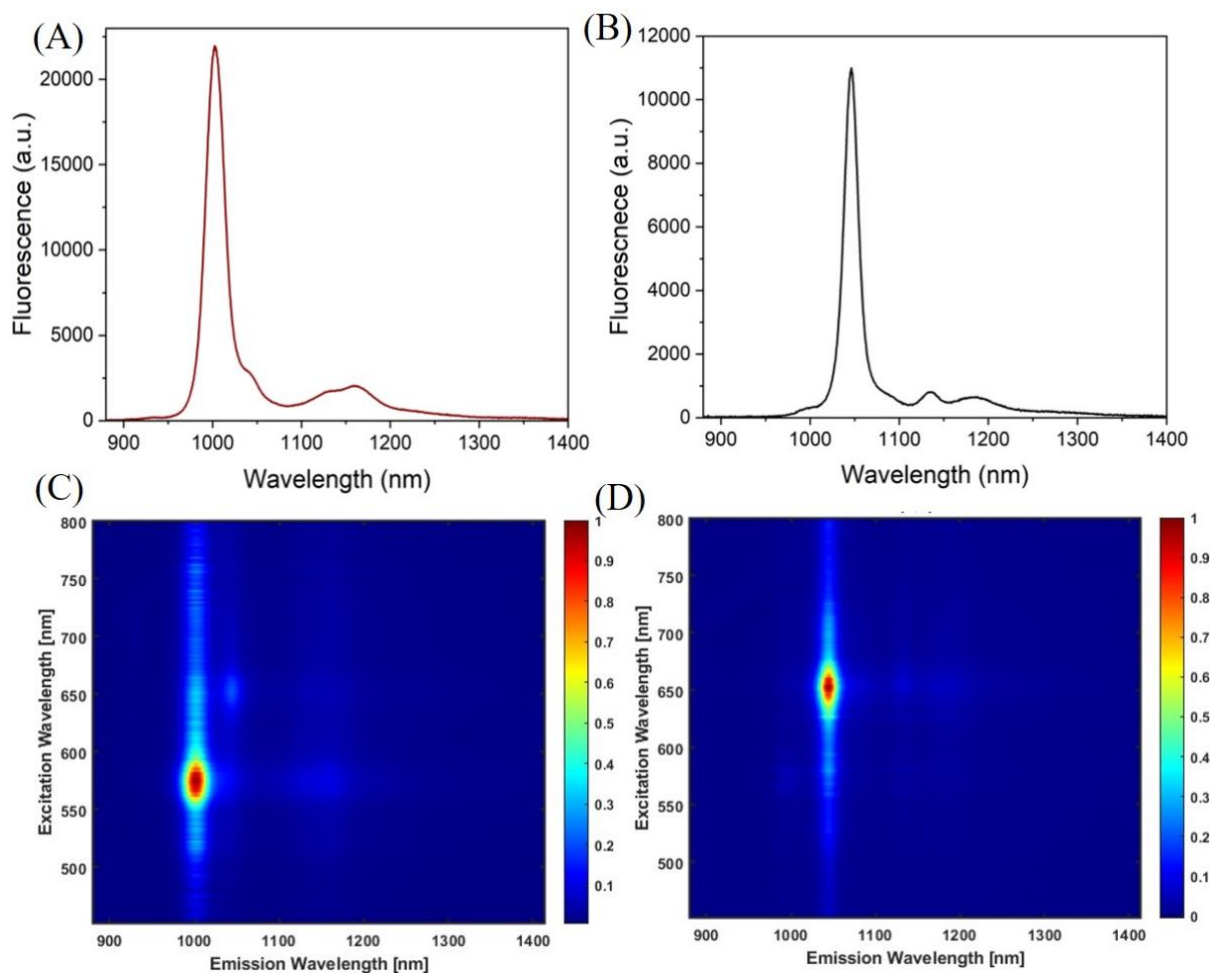


Figure S3: Fluorescence emission spectra of (A) PFO-BPy6,6' (6,5) SWCNTs upon excitation at 560 nm, and (B) PFO-FH (7,5) SWCNTs upon excitation at 650 nm, (C) excitation-emission map of (6,5) SWCNTs and (D) of (7,5) SWCNTs.

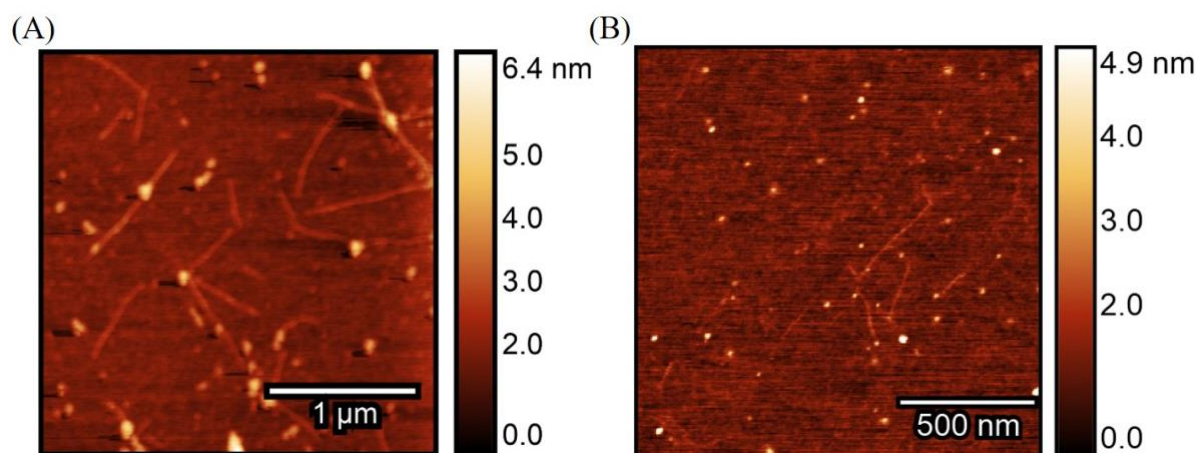


Figure S4: AFM images of (A) PFO-BPy6,6' (6,5) SWCNTs and (B) PFO-FH (7,5) SWCNTs.

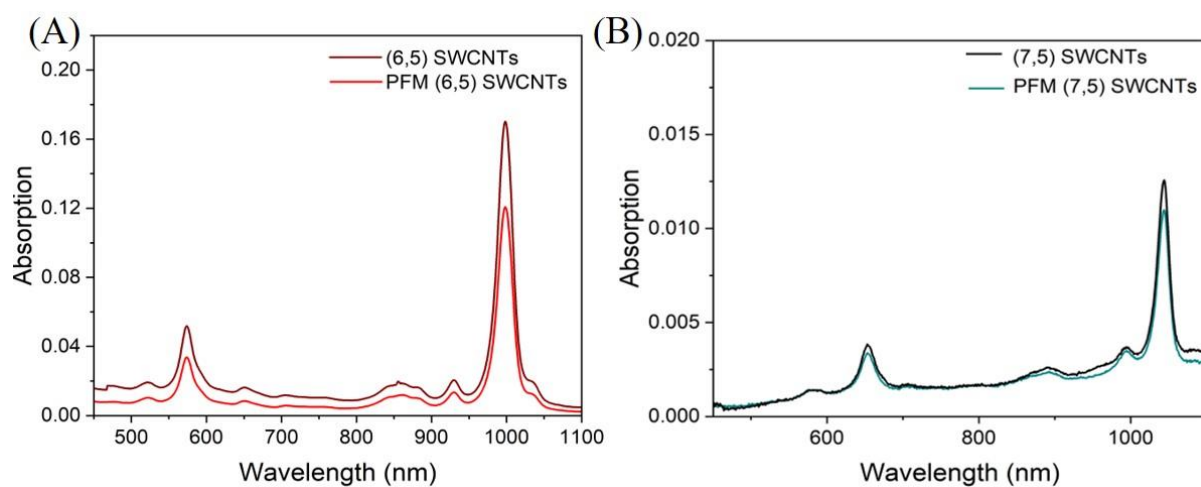


Figure S5: UV-vis-NIR absorption spectra of (A) (6,5) SWCNTs before (brown) and after (red) PFM (NaClO treatment and UV exposure), and (B) (7,5) SWCNTs before (black) and after (green) PFM.

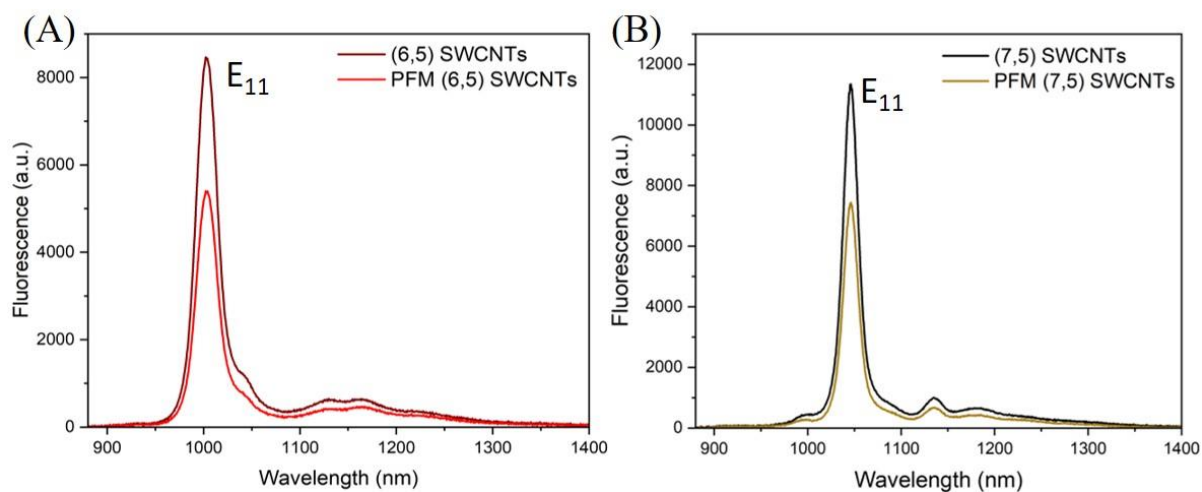


Figure S6: Fluorescence spectra of (A) (6,5) SWCNTs before (brown) and after (red) PFM, and (B) (7,5) SWCNTs before (black) and after (dark yellow) PFM.

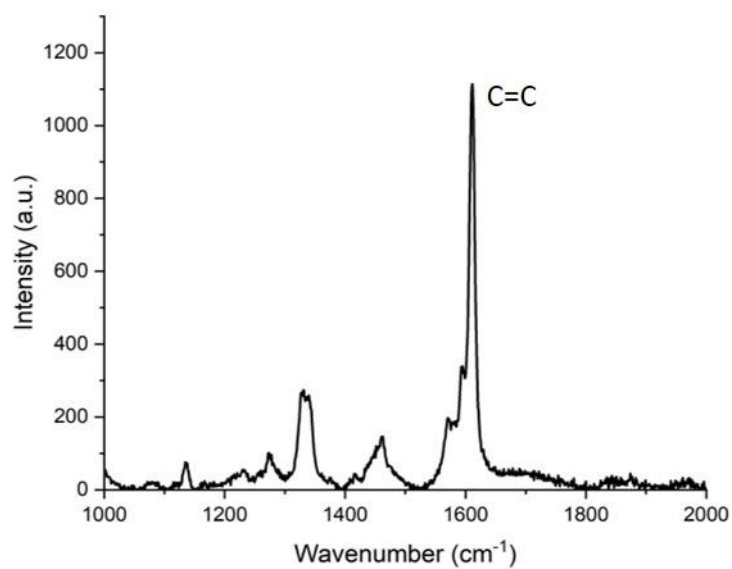


Figure S7: Raman spectrum of PFO-BPy6,6' polymer.

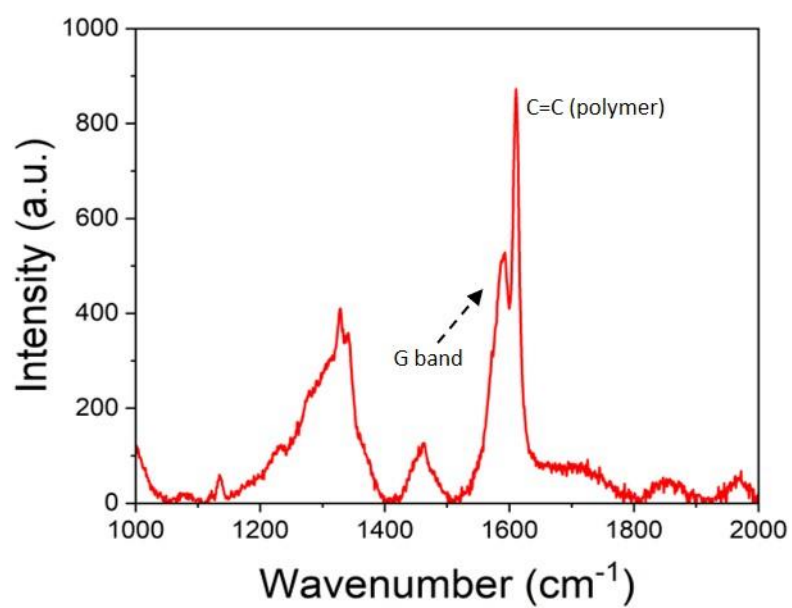


Figure S8: Raman spectrum of PFM (6,5) SWCNTs prior to polymer removal

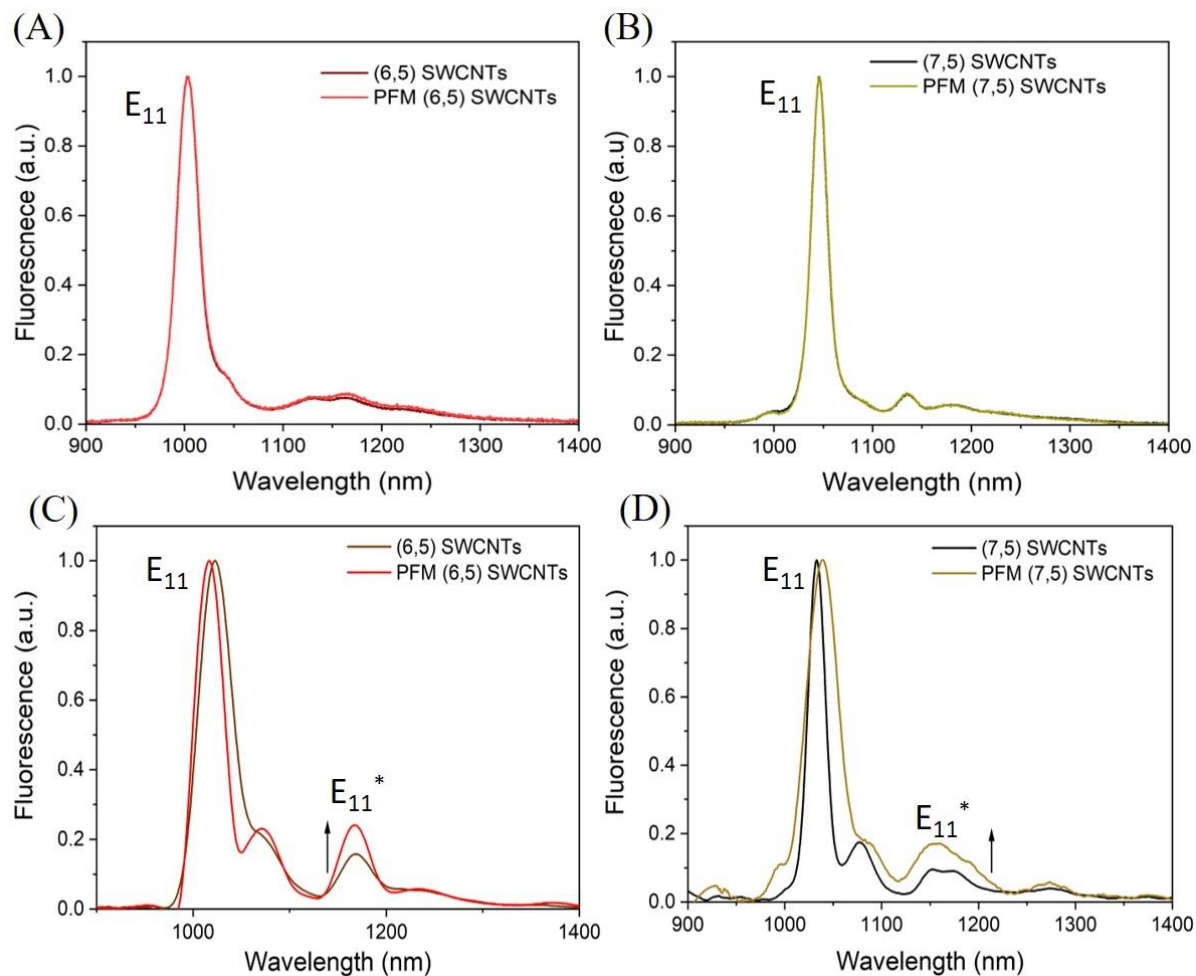


Figure S9: Normalized fluorescence spectra of (A) (6,5) and (B) (7,5) SWCNTs before and after PFM at 298 K. Normalized fluorescence spectra of (C) (6,5) and (D) (7,5) SWCNTs before and after PFM at 77 K.

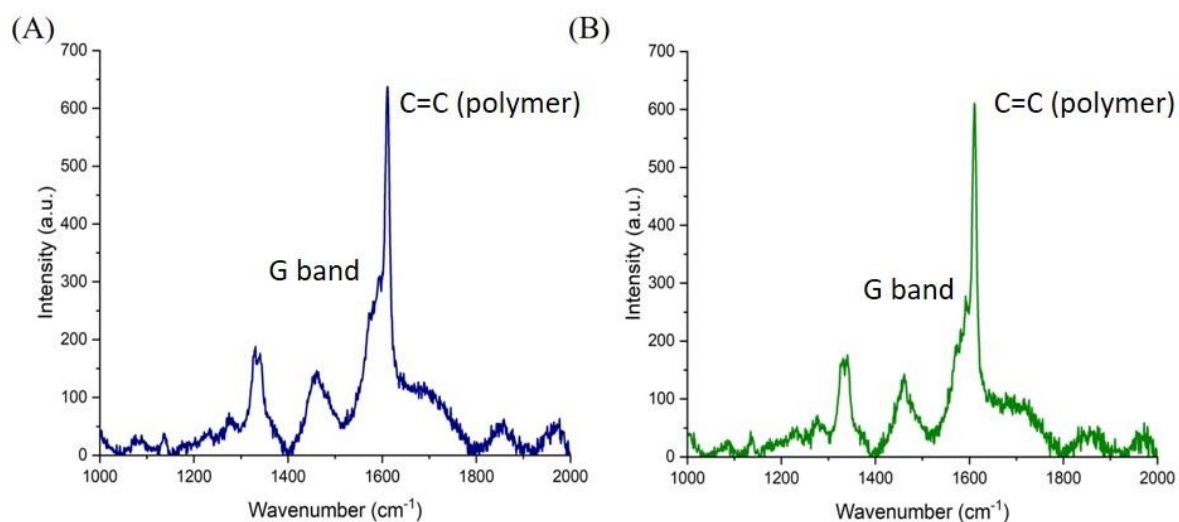


Figure S10: Raman spectra of PFO-BPy6,6' (6,5) SWCNTs upon treatment with (A) NaClO and (B) UV irradiation.

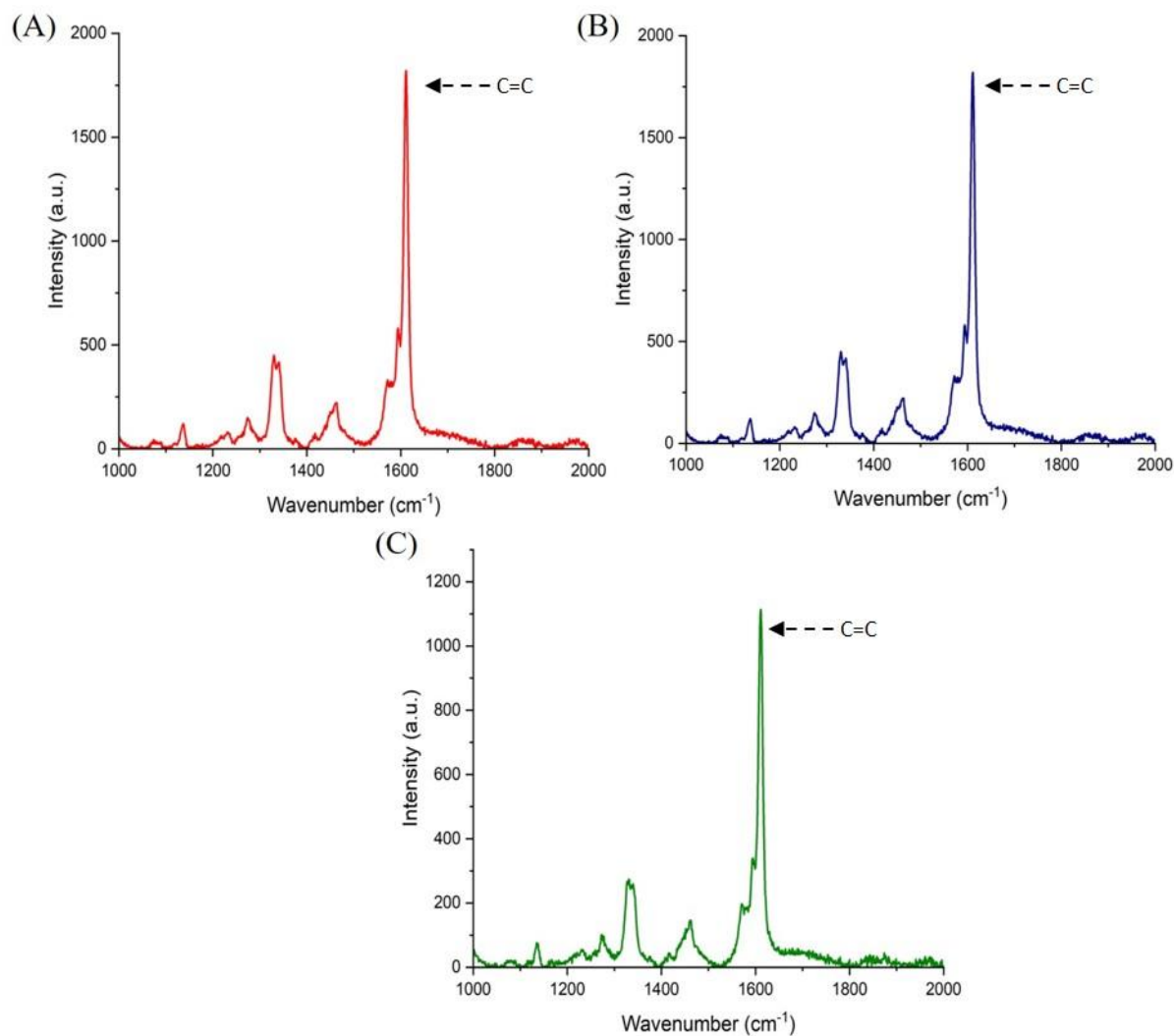


Figure S11: Raman spectra of PFO-BPy6,6' polymer upon treatment with (A) NaClO and UV irradiation, (B) NaClO, and (C) UV irradiation.

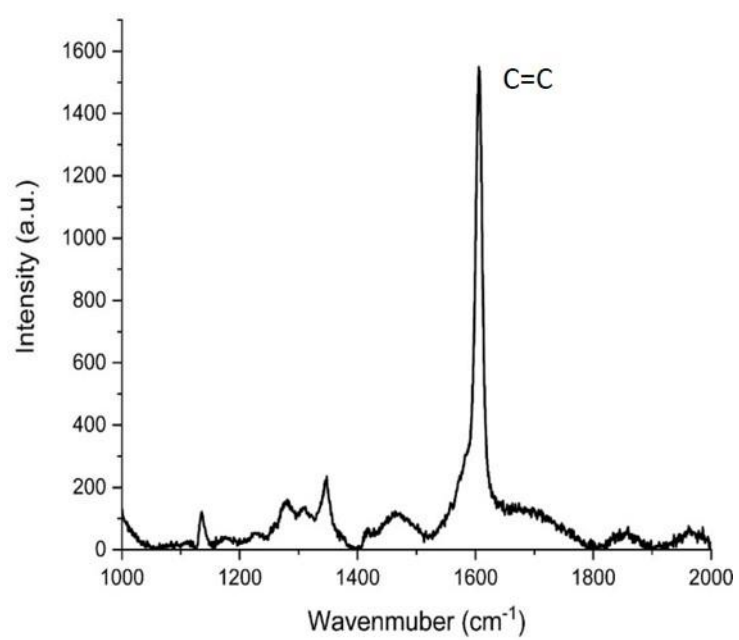


Figure S12: Raman spectrum of PFO-FH polymer.

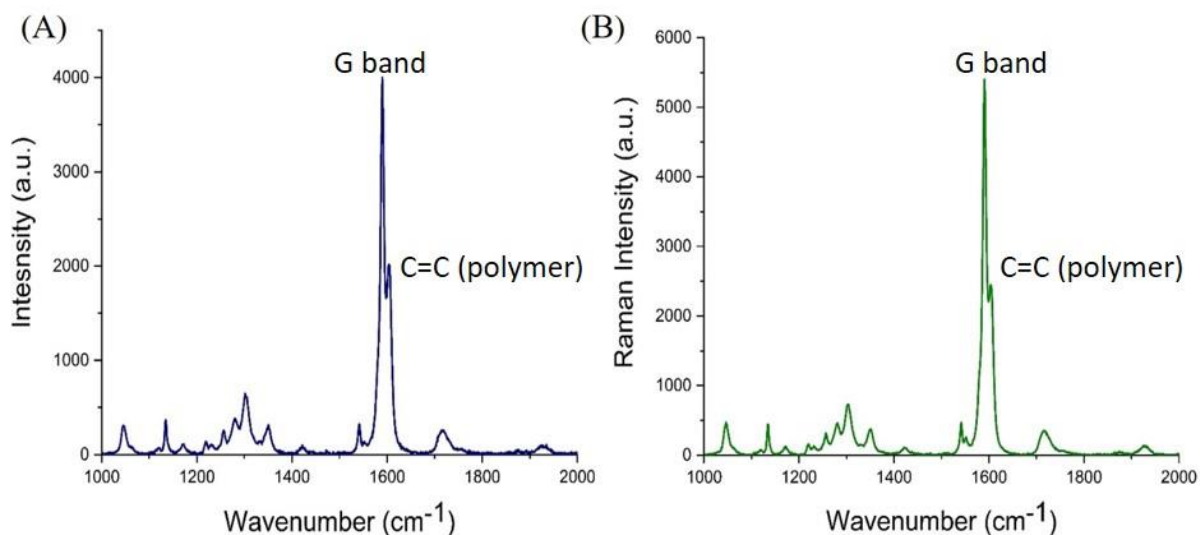


Figure S13: Raman spectra of PFO-FH (7,5) SWNCTs upon treatment with (A) NaClO and (B) UV irradiation.

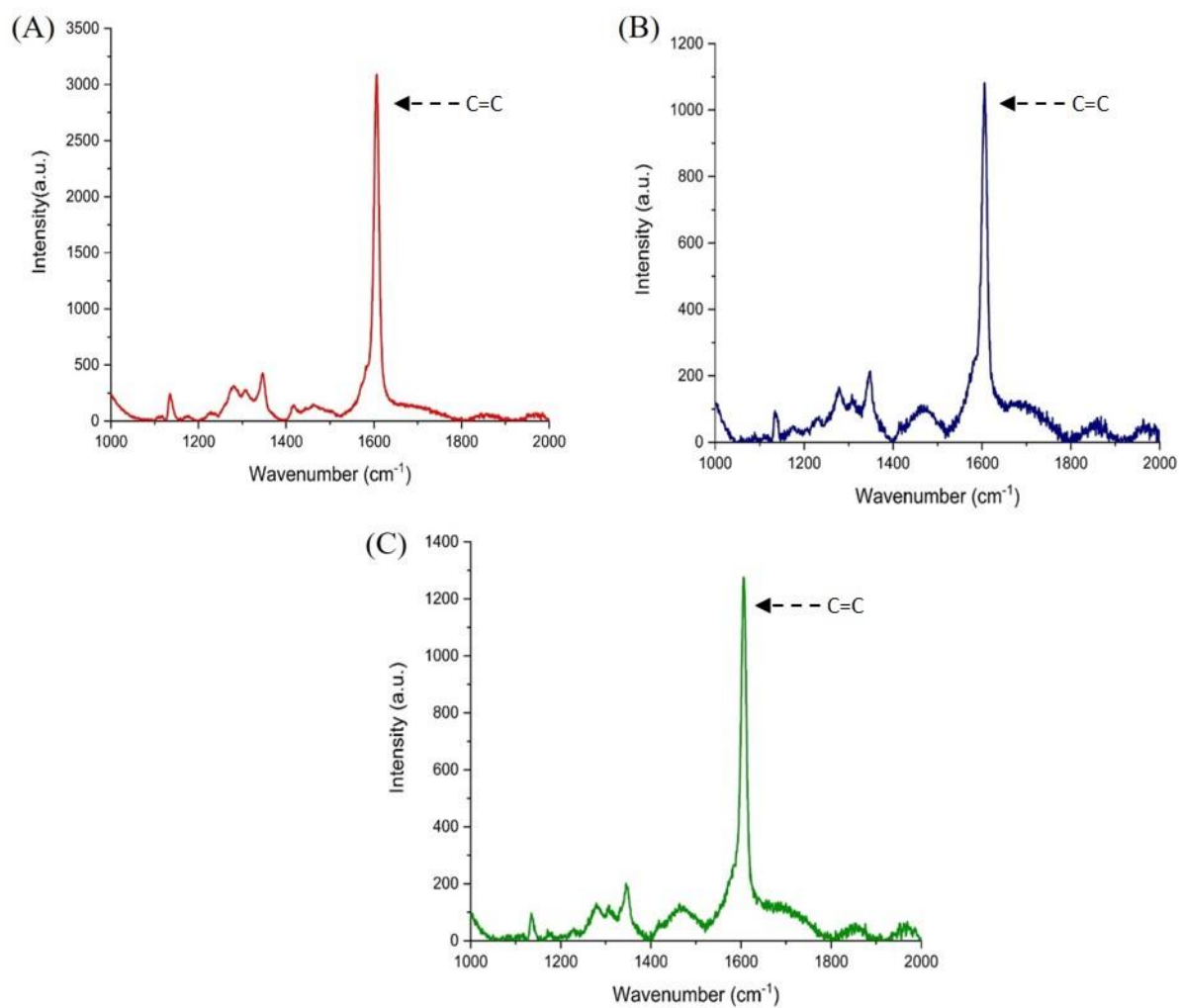


Figure S14: Raman spectra of PFO-FH polymer upon treatment with (A) NaClO and UV irradiation, (B) NaClO, and (C) UV irradiation.

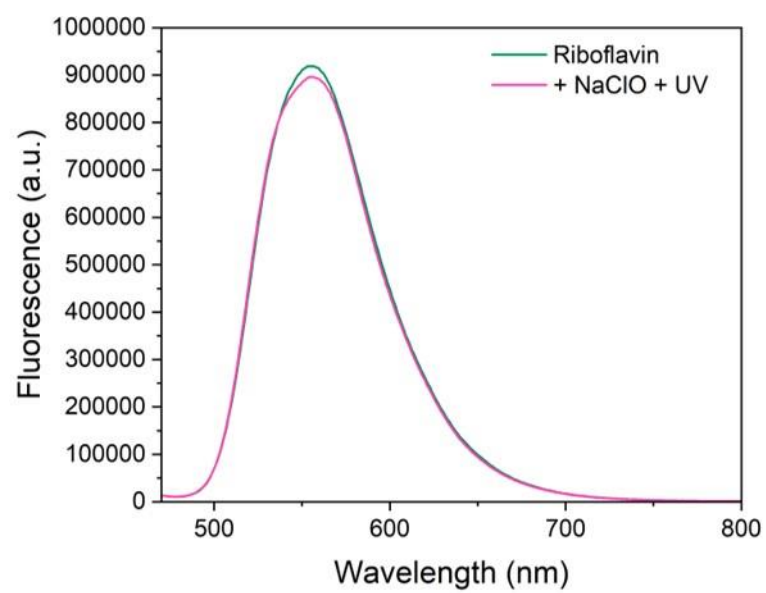


Figure S15: Fluorescence spectra of riboflavin before and after the addition of NaClO + UV exposure.

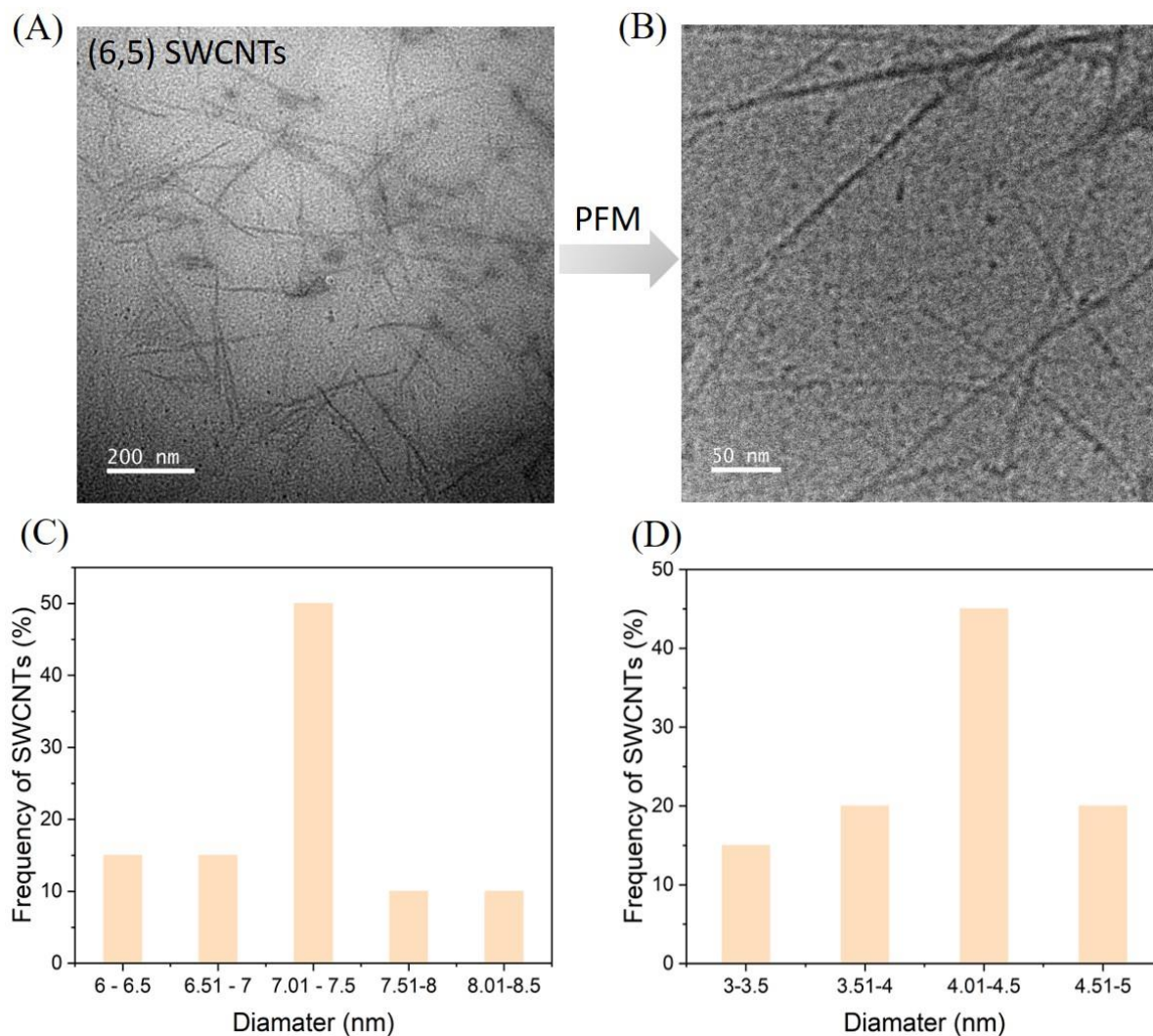


Figure S16: TEM images of (A) (6,5) SWCNTs and (B) PFM (6,5) SWCNTs. Corresponding diameter distribution histograms for the (C) (6,5) and (D) PFM (6,5) SWCNT samples.

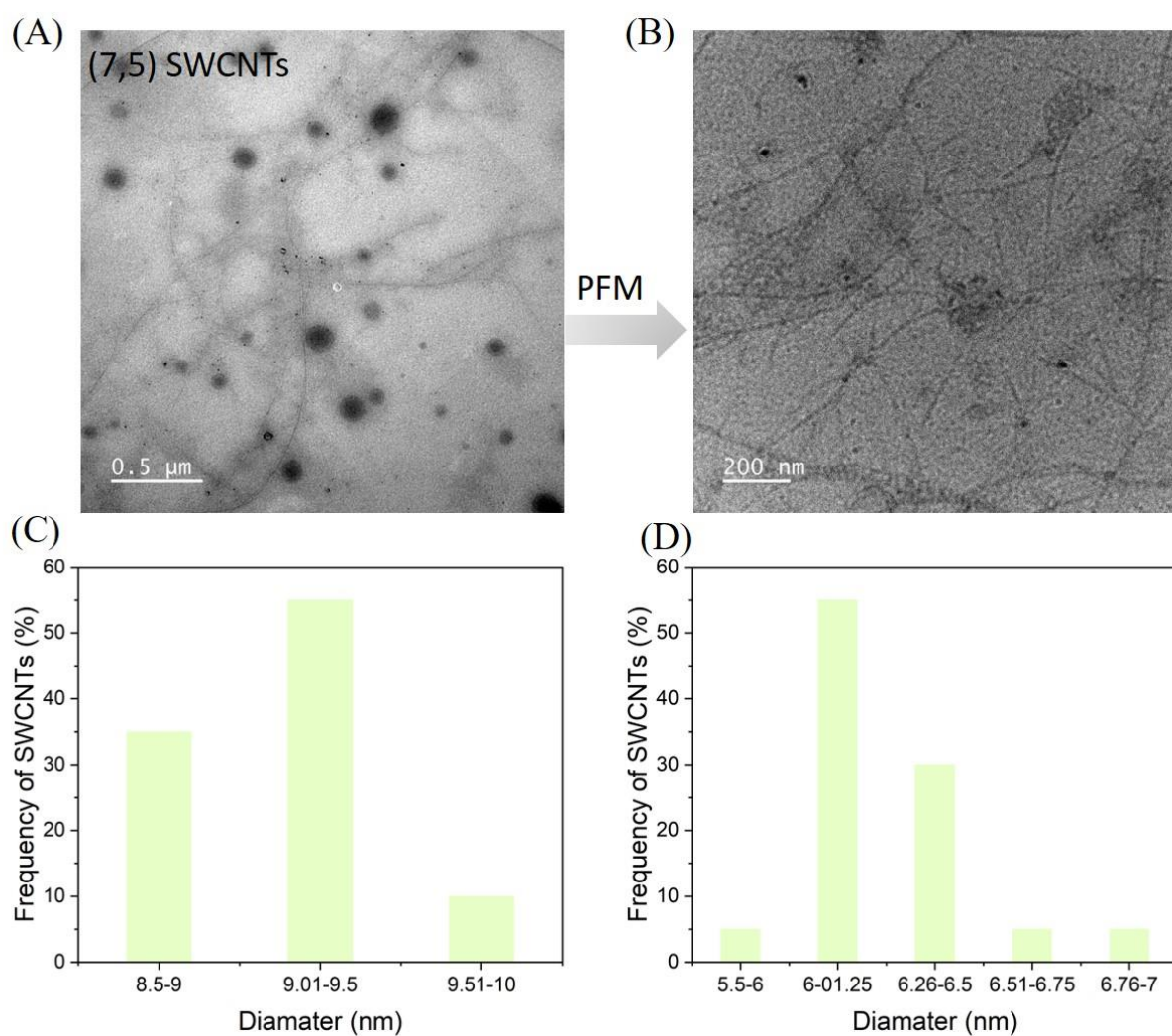


Figure S17: TEM images of (A) (7,5) SWCNTs and (B) PFM (7,5) SWCNTs. Corresponding diameter distribution histograms for the (C) (7,5) and (D) PFM (7,5) SWCNT samples.

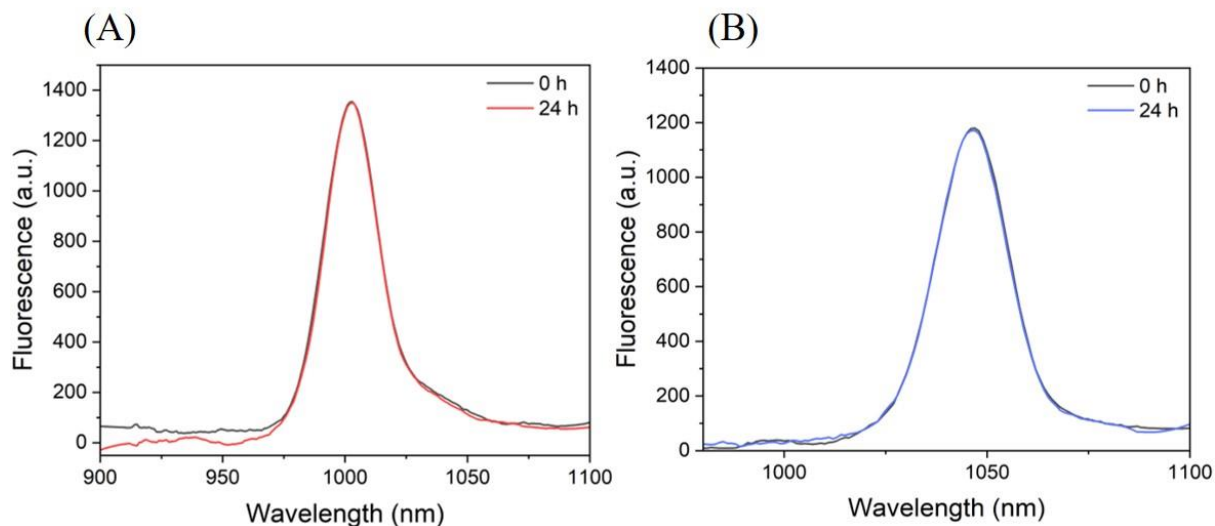


Figure S18: Fluorescence emission spectra of (A) PFM (6,5) SWCNTs and (B) PFM (7,5) SWCNTs acquired at 0 h and after 24 h.

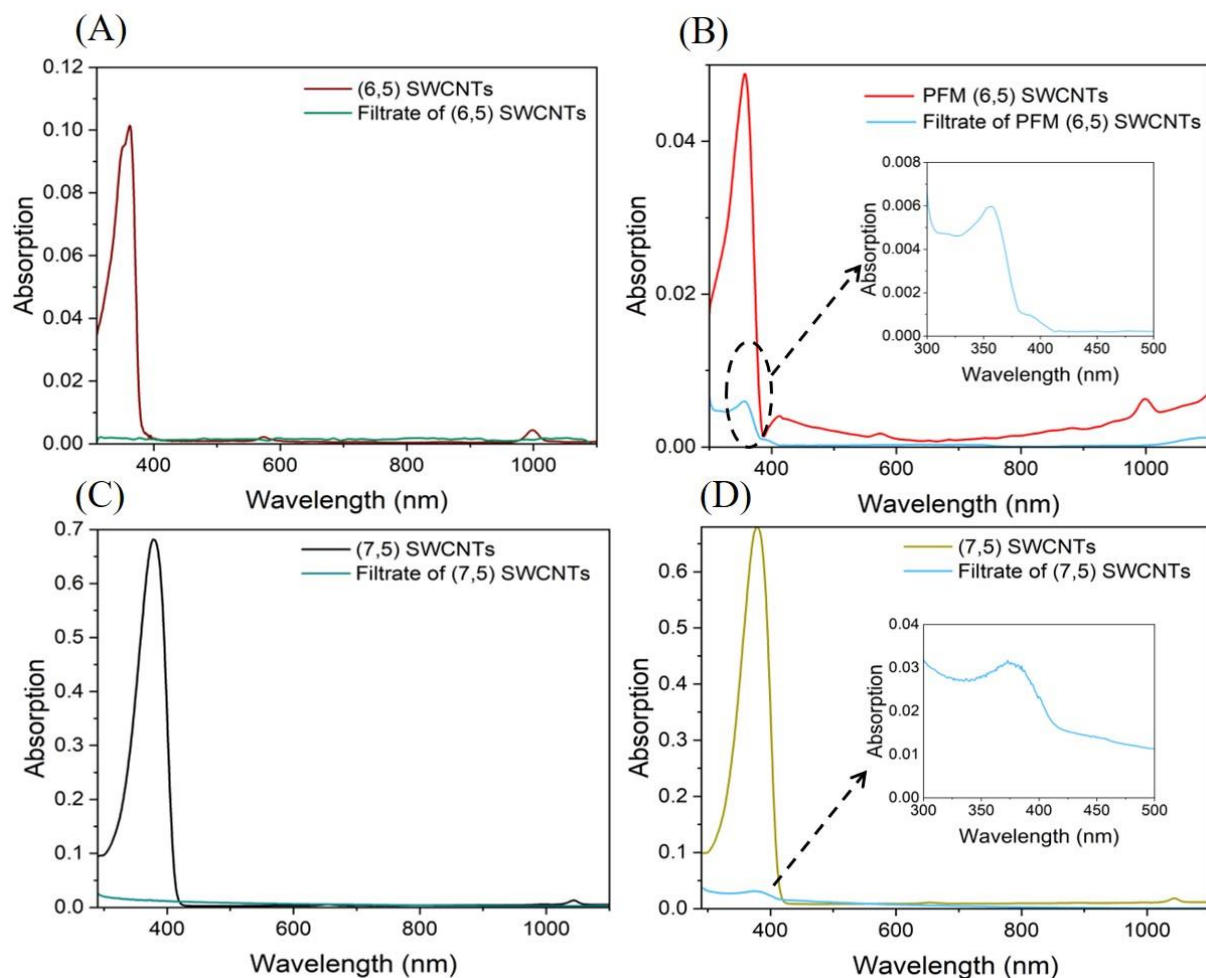


Figure S19: UV-vis-NIR absorption spectra of (A) (6,5) SWCNT suspension and its filtrate, (B) PFM (6,5) SWCNT suspension and its filtrate, (C) (7,5) SWCNT suspension and its filtrate, and (D) PFM (7,5) SWCNT suspension and its filtrate. Insets show the magnified absorption spectra of the filtrates of PFM (6,5) and (7,5) in the 300–500 nm range, respectively.

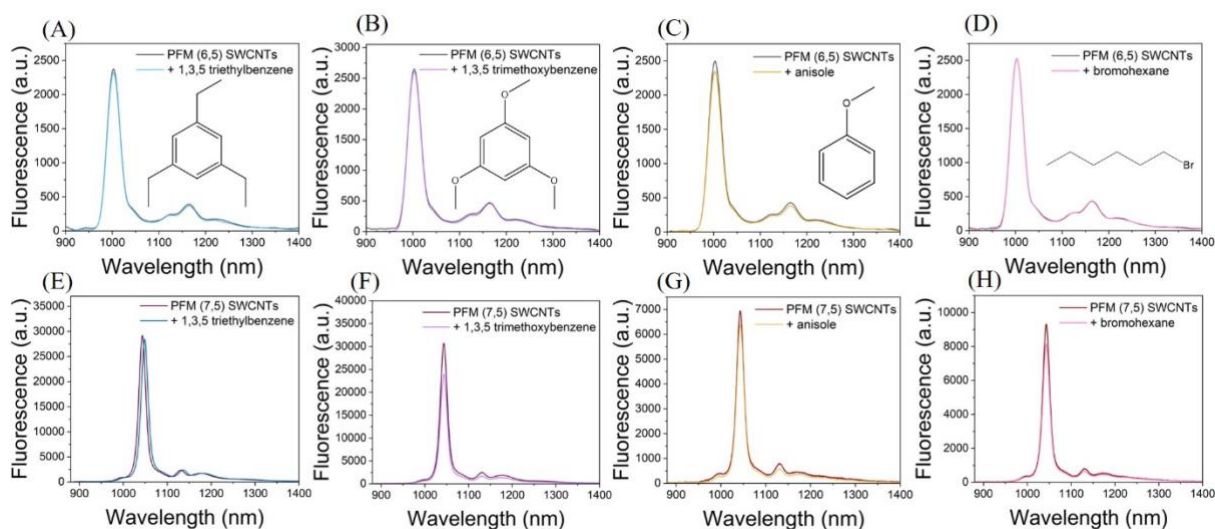


Figure S20: Fluorescence emission spectra of PFM (6,5) SWCNTs before and after the addition of 400 μM of (A) 1,3,5-triethylbenzene, (B) 1,3,5-trimethoxybenzene, (C) anisole, and (D) bromohexane. Fluorescence emission spectra of PFM (7,5) SWCNTs before and after the addition of 400 μM of (E) 1,3,5-triethylbenzene, (F) 1,3,5-trimethoxybenzene, (G) anisole, and (H) bromohexane.

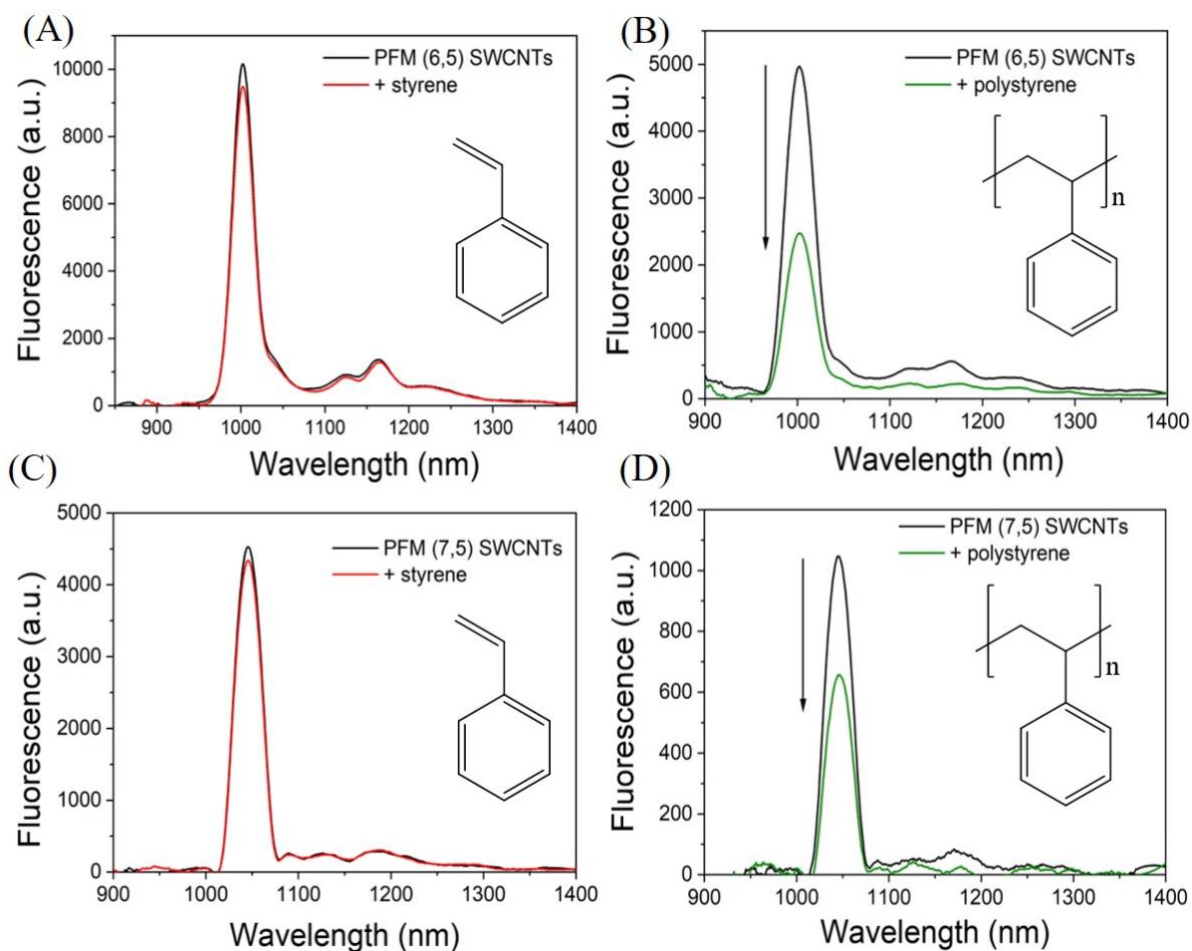


Figure S21: Fluorescence spectra of PFM (6,5) SWCNTs before and after the addition of 400 μM of (A) styrene and (B) polystyrene. Fluorescence spectra of PFM (7,5) SWCNTs before and after the addition of 400 μM of (A) styrene and (B) polystyrene.

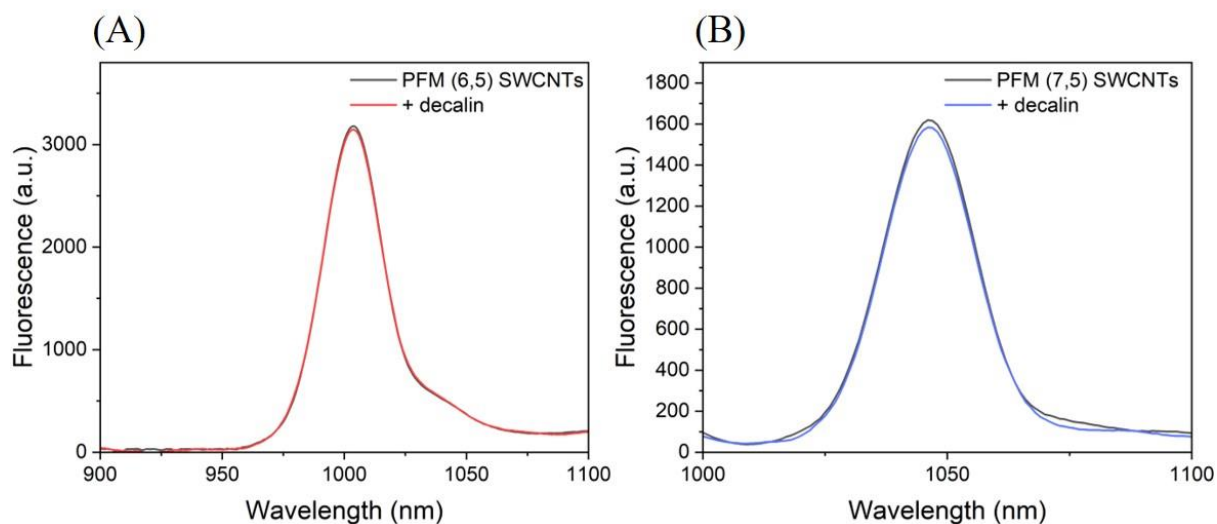


Figure S22: Fluorescence emission of (A) PFM (6,5) and (B) PFM (7,5) SWCNTs before (black) and after (red and blue, respectively) the addition of decalin.

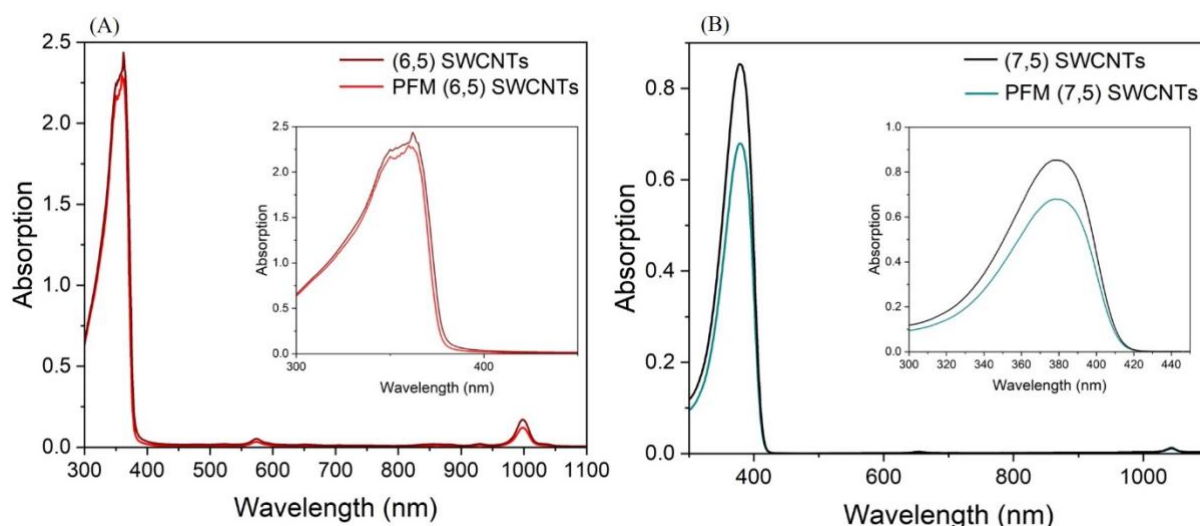


Figure S23. UV-vis-NIR absorption spectra of (A) (6,5) and (B) (7,5) SWCNTs before and after PFM treatment. Insets show the magnified 300-450 nm region, highlighting the polymer-associated peak in each case.

Table S1: Quantum yield calculation of (6,5) SWCNTs before and after the addition of PAHs

Samples	Absorption at 560 nm	Emission upon excitation at 560 nm (Area under the curve)	QY (%)
Rhodamine B	0.038595	4.22×10^6	65 (Known)
PFM-(6,5) SWCNTs	0.007138	9.50×10^3	0.79
PFM-(6,5) SWCNTs + Naph	0.012783	8.55×10^3	0.39
PFM-(6,5) SWCNTs + Phen	0.015230	6.44×10^3	0.24
PFM-(6,5) SWCNTs + Fluorene	0.019199	4.57×10^3	0.13
PFM-(6,5) SWCNTs + Pyrene	0.015230	5.57×10^3	0.22

Table S2: Quantum yield calculation of (7,5) SWCNTs before and after the addition of PAHs

Samples	Absorption at 650 nm	Emission upon excitation at 650 nm (Area under the curve)	QY (%)
Cy5	0.028083	1.51×10^6	20 (Known)
PFM-(7,5) SWCNTs	0.017519	2.20×10^4	0.52
PFM-(7,5) SWCNTs + Naph	0.013928	1.25×10^4	0.37
PFM-(7,5) SWCNTs + Phen	0.012500	1.13×10^4	0.26
PFM-(7,5) SWCNTs + Fluorene	0.013592	1.43×10^4	0.43
PFM-(7,5) SWCNTs + Pyrene	0.012339	1.16×10^4	0.39

4. References

- (1) Just, D.; Wasiak, T.; Dzienia, A.; Milowska, K. Z.; Mielańczyk, A.; Janas, D. Explicating conjugated polymer extraction used for the differentiation of single-walled carbon nanotubes. *Nanoscale Horizons* **2024**, *9* (12), 2349-2359, 10.1039/D4NH00427B. DOI: 10.1039/D4NH00427B.
- (2) Babij, N. R.; McCusker, E. O.; Whiteker, G. T.; Canturk, B.; Choy, N.; Creemer, L. C.; Amicis, C. V. D.; Hewlett, N. M.; Johnson, P. L.; Knobelsdorf, J. A.; et al. NMR Chemical Shifts of Trace Impurities: Industrially Preferred Solvents Used in Process and Green Chemistry. *Organic Process Research & Development* **2016**, *20* (3), 661-667. DOI: 10.1021/acs.oprd.5b00417.
- (3) Nagaraja, D.; Melavanki, R. M.; Patil, N. R.; Geethanjali, H. S.; Kusanur, R. A. Solvent effect on the relative quantum yield and fluorescence quenching of a newly synthesized coumarin derivative. *Luminescence* **2015**, *30* (5), 495-502. DOI: <https://doi.org/10.1002/bio.2766>.